Raman Spectroscopy of High−Pressure−High−Temperature Polymorph of Hexahydro−1,3,5−trinitro−1,3,5−triazine (ε−RDX)

ARTICLE *in* THE JOURNAL OF PHYSICAL CHEMISTRY A · JULY 2010

Impact Factor: 2.69 · DOI: 10.1021/jp102668d · Source: PubMed

2 AUTHORS, INCLUDING:

Zbigniew Dreger
Washington State University
124 PUBLICATIONS **1,126** CITATIONS

SEE PROFILE

Raman Spectroscopy of High-Pressure−High-Temperature Polymorph of Hexahydro-1,3,5-trinitro-1,3,5-triazine (ε-RDX)

Zbigniew A. Dreger* and Yogendra M. Gupta

Institute for Shock Physics and Department of Physics, Washington State University, Pullman, Washington 99164-2816

Received: March 24, 2010; Revised Manuscript Received: May 26, 2010

Raman spectroscopy was used to determine the vibrational structure and the stability of the high-pressure−high-temperature (HP−HT) polymorph of RDX after it had been quenched to room temperature. Although this polymorph has limited chemical stability under high pressure and temperature, we show that it is chemically and structurally stable from 0.6 GPa to at least 20 GPa at room temperature. Below 0.6 GPa, it readily converts to the α-polymorph. Pressure dependence of the vibrational structure of the HP−HT polymorph was measured and compared with the vibrational structures of other known RDX polymorphs: α, β, and γ. In contrast with previous suggestions, our data indicate that the HP−HT polymorph can have a different structure than the β-polymorph. This finding supports the recent suggestion that the HP−HT polymorph should be given a separate designation, ε-RDX. Furthermore, symmetry correlation analyses of Raman spectra indicate that the HP−HT polymorph (ε-RDX) may assume the space group isomorphous with the $C_{2v}[C_1(4)]$ point group and with molecules adopting the pseudo-AAA conformation.

1. Introduction

Understanding the high-pressure−high-temperature (HP−HT) response of high explosives (HEs) is important for addressing issues related to explosives sensitivity, safety, and performance. Typically, HE crystals are organic molecular solids and are often prone to high-pressure polymorphic transformations. Because different polymorphs of the same explosive can have different sensitivity to shock wave initiation, a good knowledge of the polymorphic phases is required to account for the reactive behavior of HE. For shock wave compression to result in a chemical decomposition of HE crystals, there needs to be an energy transfer to the molecules in the crystals. Although the energy transfer mechanisms have not been established, it is recognized that vibrational properties of both the crystal lattice and the individual molecules likely play an important role in this process.[1] Therefore, a detailed characterization of internal molecular vibrations and lattice vibrations of HE crystals under extreme conditions is needed.

Here we report on our work on hexahydro-1,3,5-trinitro-1,3,5-triazine, commonly known as RDX. Used extensively in explosives and monopropellants, this cyclic trimer of methylenenitramine ($(CH_2NNO_2)_3$) is an important crystalline energetic material. The present work extends our research efforts to understand the structural and chemical changes in RDX single crystals under shock wave and static compression.[2−8] Our previous experimental and computational studies have provided details on: (i) the vibrational structure of α- and γ-RDX polymorphs under static compression,[2,3] (ii) the α → γ phase transition under static and shock compression,[2−4] (iii) the HP−HT phase diagram of RDX,[6] and (iv) shock-wave induced decomposition.[7,8]

The focus of this article is on the vibrational structure of the HP−HT polymorph of RDX to resolve some long-standing scientific issues.

Several RDX polymorphs have been reported to occur under a variety of conditions.[2,9−19] It has been well established that at room temperature RDX can exist in two stable polymorphs: (i) the α-RDX up to 3.8 GPa with an orthorhombic *Pbca* structure and eight molecules per unit cell,[9,10] and (ii) the γ-RDX above 3.8 GPa, with an orthorhombic $Pca2_1$ structure and eight molecules in the unit cell.[12] Consequently, the α−γ transition was found to involve a decrease in volume of about 3% and a change in the molecular conformations. Specifically, all molecules in α-RDX adopt the so-called AAE-chair conformation, in which two of the NO_2 groups are in pseudoaxial positions and the other is in a pseudoequatorial position with respect to the s-triazine ring. However, in the case of γ-RDX, two adjacent molecules adopt two different conformations: AAA and AAI where 'I' represents an intermediate orientation of the NO_2 group with respect to the s-triazine ring. Recently, FTIR measurements have suggested that another polymorph, termed tentatively as δ-RDX, of unknown structure, can occur above ∼18 GPa.[13]

Furthermore, early studies reported that a highly metastable form of RDX can be obtained in microscopic quantities by evaporation of high-temperature boiling solutions containing RDX; this polymorph was termed β-RDX.[9,14,15] More recently, this metastable form was produced by the deposition of RDX from acetonitrile solution on a glass substrate.[16] Despite the metastability of β-RDX, information on its vibrational structure was gathered. Similarity between the experimental vibrational spectra[16] and the density functional theory (DFT) calculations for a single molecule[16,20,21] indicated that molecules in this polymorph may adopt the AAA conformation. Subsequent X-ray diffraction studies confirmed this molecular conformation and determined the crystal structure. It was found that β-RDX has the same space group as γ-RDX.[17]

Optical spectroscopy studies using Raman[18] and FTIR[19] measurements demonstrated that both α- and γ-RDX transform to another RDX polymorph at elevated temperatures. On the basis of some similarities in vibrational spectra, these studies suggested that this HP−HT polymorph adopts the same structure

* Corresponding author. E-mail: dreger@wsu.edu. Tel: 509-335-4233. Fax: 509-335-6115.

10.1021/jp102668d
Published on Web 06/10/2010

as β-RDX. Therefore, it was proposed that the HP−HT polymorph is actually the β-RDX. Our recent work has shown that the HP−HT polymorph can only be formed in a limited range of pressures and temperatures, and it is chemically unstable in the pressure−temperature domain where it is produced.[6] Therefore, obtaining reliable information on the structural properties of the HP−HT polymorph is challenging. Despite this difficulty, it was recently suggested that the HP−HT polymorph may actually have a different structure than the β-polymorph.[6,17] Because this polymorph is formed at the pressure and temperature conditions encountered under shock wave initiation, it is important to identify its vibrational and structural properties for understanding shock-induced decomposition of RDX.

The present work builds on the fact that the transformation of α- or γ-RDX to the HP−HT polymorph is irreversible, and this polymorph can be quenched to room temperature,[6,18,19] allowing its detailed investigation. Using high-pressure Raman spectroscopy measurements, we provide comprehensive information on the vibrational structure of the HP−HT polymorph. The specific objectives of this work were: (1) to produce a stable HP−HT RDX polymorph and to determine the details of its vibrational structure, (2) to examine its pressure stability, and (3) to assess the previously proposed association of the HP−HT polymorph with β-RDX. It is also our intent to provide comprehensive experimental data for future theoretical studies on the HP−HT polymorph.

The remainder of the article is organized as follows. Experimental procedures including sample preparation, high-pressure generation, and Raman measurements are briefly described in the next section. Section 3 presents experimental data and discussion regarding: (i) the pressure dependence of the internal and external vibrations of the HP−HT polymorph, (ii) the differences and similarities between the vibrational spectra of the HP−HT polymorph and the α-, γ-, and β-polymorphs, and (iii) a possible structure of the HP−HT polymorph. The main findings of this work are summarized in Section 4.

2. Experimental Procedures

Grains of single crystal RDX were obtained from Dr. D. E. Hooks of Los Alamos. The crystals were carefully selected based on quality and size. An optical microscope (160×) was used to select crystals free of microscopic defects. The crystals were further selected to ensure that the samples occupied only a fraction of the high-pressure cell compartment. Typical crystals did not exceed 0.12 mm on a side and 0.03 mm in thickness. To facilitate a comparison of the HP−HT and β-polymorphs, we also prepared β-RDX as deposits from acetonitrile solution and single crystals from highly concentrated nitrobenzene solutions, according to the procedures reported in refs 16 and 17, respectively.

High pressure was generated using a modified Merrill-Bassett type diamond-anvil-cell (DAC). A stainless-steel gasket, pre-indented to 0.08 mm with a 0.2 mm hole drilled in the indentation, served as the sample compartment. Cryogenically loaded argon was used as a pressure-transmitting medium. Note that the cryogenic loading did not affect the crystal quality. Ruby fluorescence was used to monitor pressure,[22] determined from the frequency shift of the R-lines of the ruby crystal. By monitoring the separation and widths of both the R_1 and R_2 lines, we confirmed that no significant change in these parameters was observed up to 15 GPa. Therefore, quasi-hydrostatic conditions were maintained up to 15 GPa. The precision of our pressure measurements was estimated to be 0.05 GPa. To produce the HP−HT polymorph, the DAC was heated with a resistive heater wrapped around the cell. The temperature of the sample was monitored with iron−constantan thermocouples. The accuracy of temperature measurements was determined to be ±2 K.

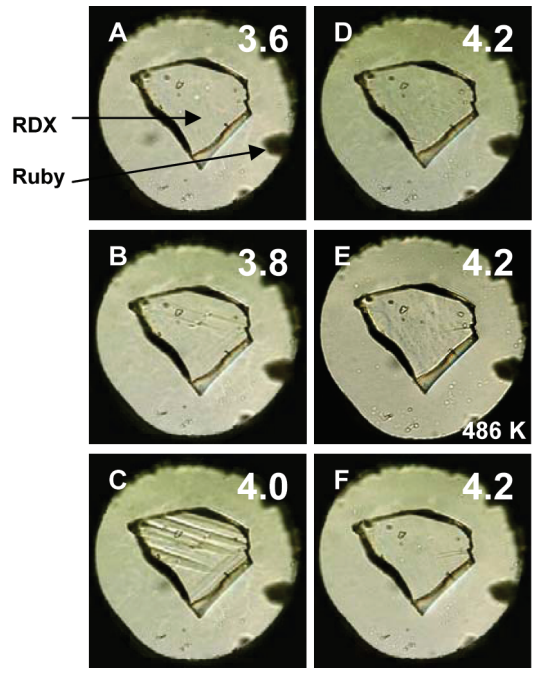

Figure 1. Images of different polymorphic phases of RDX in a diamond anvil cell: (A) α-RDX, 3.6 GPa at room temperature (RT); (B) α-RDX, 3.8 GPa at RT; (C) α-RDX, 4.0 GPa at RT; (D) γ-RDX, 4.2 GPa at RT; (E) HP−HT-RDX, 4.2 GPa at 486 K; (F) HP−HT-RDX, 4.2 GPa at RT. Note that the color is artificial because the RDX crystal is colorless.

The 532 line from a cw diode-pumped solid-state (DPSS) laser (Verdi-Coherent) was employed for Raman excitation. A micro-Raman system (T64000, JY-Horiba) equipped with a microscope (Olympus BX-40) was used; it provided a spectral resolution of ∼0.8 cm^{-1} and a spatial resolution of 5 μm. The micro-Raman system was capable of measuring spectra to frequencies as low as 20 cm^{-1}. Less than 50 mW of power was used to avoid any damage to the sample. The crystals used in these studies had a random orientation with respect to the excitation beam. Raman spectra measurements were performed up to 20 GPa. The Raman spectra were not corrected for the spectral sensitivity of the detection system. Pressure-induced shifts of overlapping bands were analyzed by fitting the Raman spectra to a Voigt (Gaussian−Lorentzian) function using a nonlinear least-squares algorithm. Experimental details regarding our Raman and ruby fluorescence techniques can be found elsewhere.[2,23]

3. Results and Discussion

3.1. Preparation of the Stable HP−HT Polymorph. As we have shown elsewhere, the HP−HT polymorph has limited chemical stability under the pressure−temperature conditions where it is produced.[6] However, in the present work, we found that this polymorph can be quenched to a stable form by decreasing the temperature. In Figures 1 and 2, we demonstrate that this procedure can indeed preserve both the quality of the single crystal and the vibrational structure of the high-temperature phase. Specifically, in Figure 1, we show changes in the crystal's appearance and quality over the course of the polymorphic transformations. Images A, B, and C represent α-RDX

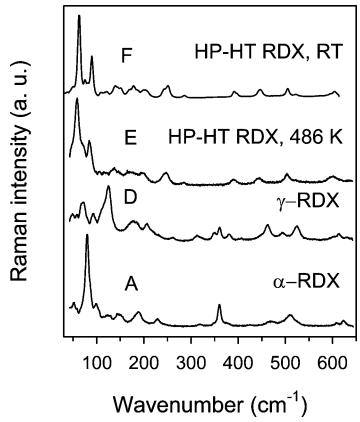

Figure 2. Low-frequency Raman spectra of different polymorphic phases of RDX offset vertically. The symbols next to each spectrum correspond to symbols and descriptions in Figure 1. Spectra A, D, and E were acquired for 10 s, whereas the spectrum F was acquired for 30 s.

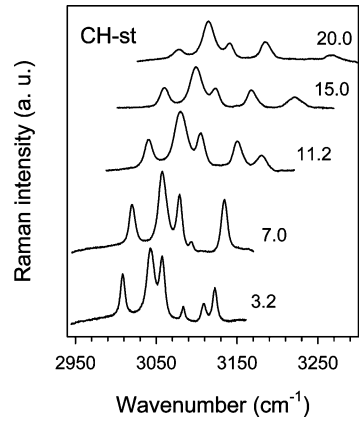

Figure 3. Raman spectra of the CH stretching modes at several pressures. Pressure values in gigapascals are shown next to each spectrum.

at pressures 3.6, 3.8, and 4.0 GPa, respectively, just near the expected $\alpha \rightarrow \gamma$ phase transition at room temperature. The formation of parallel lines on the crystal surface can be seen at the onset of the phase transition at 4.0 GPa.

Although the phase transition involves a volume change of 3%,[12] the crystal remains intact with "wrinkles" on the crystal disappearing as the pressure is increased to 4.2 GPa. At this pressure, the crystal is in the γ-phase, as seen by comparing the Raman spectra labeled A (α-RDX) and D (γ-RDX)[2] in Figure 2. Heating the crystal at this pressure with a rate of 1 to 2 K/min transforms the crystal almost instantaneously from the γ-polymorph to the HP−HT polymorph upon reaching 486 K. This can be seen in the characteristic changes in the Raman spectrum (spectrum E, Figure 2). Subsequent cooling to room temperature preserves the vibrational structure of the HP−HT phase, as evidenced by the similarity between spectra E and F in Figure 2. It is worth noticing that the high-temperature spectrum (E) is less resolved than the room-temperature spectrum (F), likely because of the thermal effects.

A comparison of images D, E, and F in Figure 1 clearly demonstrates that neither the $\gamma \rightarrow$ HP−HT transition nor the subsequent cooling affects the crystal quality. In contrast, we found that other pressure-transmitting media (such as nitrogen or a methanol/ethanol mixture (4:1))[17,18] do not preserve crystal quality and integrity; the crystal was shattered in nitrogen and dissolved in the M/E mixture. Therefore, we used argon as a pressure-transmitting medium. Because this medium does not affect crystal quality during the phase transitions, it provides more reliable data than previous studies on RDX.[17,18]

Below, we present the results of pressure effects on the HP−HT polymorph quenched to room temperature. Raman spectra were measured during pressure increase from 4 to 20 GPa and from 4 GPa to ambient pressure in two separate runs. One experiment was also performed on the same sample upon increase and decrease of pressure. No measurable hysteresis in Raman shifts was observed in this experiment. Because the vibrational spectra of the crystal quenched to room temperature are identical to the spectra of the crystal at high temperature, we use the same nomenclature for the room-temperature polymorph as for the high temperature: the HP−HT polymorph.

3.2. Pressure Effects on Raman Modes of the HP−HT Polymorph. ***3.2.1. Frequency Range 3300−2900 cm^{-1} (CH_2 Stretching Modes).*** Figures 3 and 4 show pressure-induced changes in the CH-stretching modes (symmetric and asymmetric). Six modes are predicted in this range, and all are observed experimentally. With increasing pressure, all modes shift gradually toward higher frequencies but at different rates. The differences in the pressure shifts ultimately lead to larger separation, crossing, or overlapping of some peaks. Of particular interest in this frequency range are: (i) the crossing of the two highest frequency peaks, ν_1 and ν_2, (ii) fading of the ν_3 mode, and (iii) the broadening of all modes at pressures above ~15 GPa. In the case of the ν_1 and ν_2 modes, substantially different pressure shifts lead to the crossing of these modes at 7 to 8 GPa, followed by their increased separation at higher pressures (inset, Figure 4). This behavior is quite similar to that observed for the same modes of the α-polymorph. In the latter, however, the crossing of modes took place at lower pressures. The weak intensity ν_3 mode does not disappear with increasing pressure but is buried under the strong peak of the ν_4 mode. The broadening of peaks at higher pressures is likely caused by nonhydrostatic conditions occurring above 15 GPa, as determined from the changes in the ruby lines splitting.

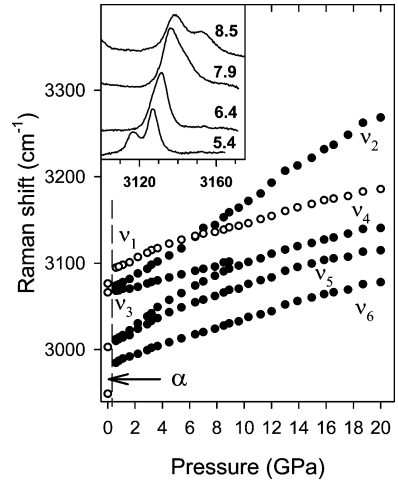

Figure 4. Pressure-induced shifts for CH-stretching modes. The mode ν_1 is presented by open symbols. The vertical dashed line marks the onset of the transition from the HP−HT polymorph to the α-polymorph upon pressure unloading. Prime symbol denotes modes that either overlap with other modes at 0.6 GPa or show up at higher pressures. Inset presents details of evolution with pressure for modes located at 3095 and 3074 cm^{-1} at 0.6 GPa. In this and other graphs representing the Raman shifts, the error bars are smaller than the plotting points.

Apart from a general increase in frequencies at higher pressures, there are no other apparent changes in the spectra up to 20 GPa. The gradual shifts indicate that the HP−HT

TABLE 1: Frequencies and Pressure Dependence of Raman Modes of the HP−HT RDX Polymorph[a,b]

mode	HP−HT RDX				β-RDX		
	freq. (cm^{-1}) ± 0.5	tentative assign.	$d\nu/dp$ (cm^{-1} GPa^{-1}) ± 0.1		this work	ref 16	
			at 0.6 GPa	at 20 GPa	freq. (cm^{-1}) ± 0.5	freq. (cm^{-1})	assign.
ν_1	3095	CH st	6.1	3.1	3081	3075.1	C−H st
ν_2	3074	CH st	10.5	10.4	3070	3066.5	C−H st
ν_3	3068	CH st	3.7				
ν_4	3012	CH st	11.9	1.1			
ν_5	3010	CH st	8.2	2.6	2992	2987.0	C−H st
ν_6	2985	CH st	5.8	3.9			
ν_7	1592	O−N−O st	3.5	2.2	1597	1590.9	N−O st
ν_8	1578	O−N−O st	3.0	1.9	1578	1574.3	N−O st
ν_9	1569		2.7	1.6	1559		
ν_{10}	1541	O−N−O st	3.0	2.4		1547.9	N−O st
ν_{11}	1520		2.0	1.1	1509	1507.2	N−O st
ν'_{11}	1520		2.0	0.8			
ν_{12}	1450	N−N st	2.0	1.4	1446	1442.7	C−H skl
ν'_{12}	1446 (3.2)			0.9			
ν_{13}	1427	N−N st	2.5		1421	1419.5	C−H skl
ν'_{13}	1438 (8.9)						
ν_{14}	1422	N−N st	1.3	0.5			
ν_{15}	1375	N−N st	2.6	1.8	1376	1373.8	CH_2 sci
ν_{16}	1374	N−N st	1.6	2.5			
ν'_{16}	1376 (8.5)	N−N st		2.2			
ν_{17}	1278	CH_2 wag	5.1				
ν_{18}	1272	CH_2 wag	3.8		1273	1271.9	N−O st
ν_{19}	1263	CH_2 wag	3.5		1263	1261.4	N−N st
ν_{20}	1209	CNC st	4.0	1.7	1226		
ν_{21}	1195	CNC st	4.0	1.5	1211	1211.1	CH_2 wag
ν_{22}	1095	CNC st	4.0	3.2			
ν_{23}	995	CH_2 r	2.0		999	996.7	ring st/N−N st
ν_{24}	937	CH_2 r	5.5	1.7	933/940	932.8	ring st
ν_{25}	920	CH_2 r	5.2	2.3			
ν_{26}	910		4.9	1.3			
ν_{27}	883	CH_2 r	3.5	2.1	880	878.8	ring breath
ν_{28}	854	CN st	3.8	1.5			
ν_{29}	851	ring CNC st	3.5	1.9	849	849.0	CH_2 r
ν_{30}	793	ring CNC st	3.0	0.9	789	787.5	ring st/NO def
ν_{31}	786	ring CNC st	2.6	0.6			
ν_{32}	761	ring CNC st	0.9	0.4	755	754.7	
ν'_{32}	763 (2.2)			0.4			
ν_{33}	726	N−NO_2 u	−2.6	0.7	733	733.0	C−N−C def
ν'_{33}	726 (2.2)			0.6			
ν_{34}	667 (0.8)	ring b		1.3			
ν'_{34}	661		3.0	1.2	656	657.5	
ν_{35}	591	ring tw	3.9	2.1	589	588.8	
ν_{36}	582	ring tw	3.9	1.9			
ν_{37}	509	ring tw	3.7	1.6	504	504.3	
ν_{38}	488	ring tw	4.8	2.5	480/473	479.7	
ν_{39}	433	ring b	3.5	1.7	425	424.2	ring breath
ν'_{39}	443 (3.2)			1.9			
ν_{40}	382	N-NC_2 u	3.6	0.3	376	376.8	C−N−C def
ν'_{40}	390 (2.9)			0.9			
ν''_{40}	412 (8.5)			1.8			
ν_{41}	282	ring st	−1.3	2.5	248		
ν_{42}	236	N-NC_2 u	4.4	3.3	228	227.3	
ν_{43}	231	N-NC_2 u	4.1	3.6	217		
ν_{44}	163	NO_2 rot	14.1	3.6			
ν'_{44}	194 (3.2)			1.0			
ν_{45}	153	NO_2 rot	10.7	3.0	153		
ν_{46}	142	NO_2 rot	12.0	2.6			
ν_{47}	108	NO_2 wag	13.1	2.4			
ν_{48}	102	NO_2 wag	13.5	2.9	102		
ν_{49}	100 (1.6)	lattice		2.0	92		
ν_{50}	93 (1.6)	lattice		1.2	85		
ν_{51}	64	lattice	11.2	2.3			
ν'_{51}	94 (4.5)	lattice		2.8	76		
ν_{52}	49	lattice	11.1	2.2	52		
ν_{53}	45	lattice	9.5	2.6	40		
ν_{54}	41	lattice	7.2	0.3			
ν'_{54}	72 (6.4)	lattice		0.9			
ν_{55}	32	lattice	8.9		30		

[a] Data for β-RDX are from this work and also adopted from ref 16. [b] Modes that occur at higher pressure than 0.6 GPa are denoted with prime symbol, and their pressure onsets are given in brackets. Abbreviations: st = stretch, skl = skeletal, sci = scissor, wag = wagging, r = rock, b = bend, tw = twist, u = umbrella, rot = rotation, def = deformation. Note that the values of $d\nu/dp$ are not given in the Table if the mode was not measured at the specified pressures. The modes in the spectral range from 1280 to 1370 cm^{-1} are not listed because they were not accessible in experiments with a diamond anvil cell.

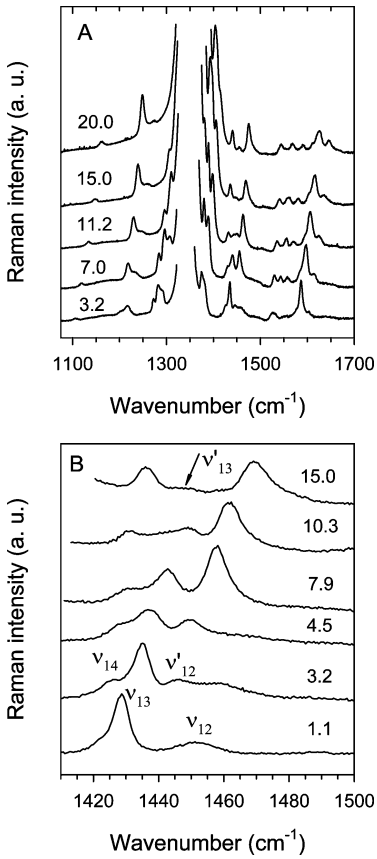

Figure 5. (A) Raman spectra in the frequency range 1100−1700 cm^{-1} at several pressures. The gap in the spectra corresponds to the removed Raman mode of diamond (∼1332 cm^{-1}). (B) Details of evolution of N−N stretching modes (1400−1500 cm^{-1}) with pressure.

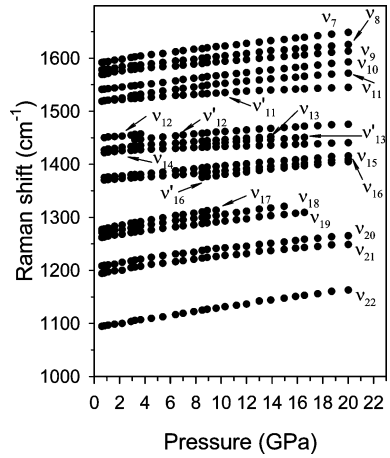

Figure 6. Pressure-induced shift of Raman modes between 1100 and 1700 cm^{-1}. Modes located in the neighborhood of 1332 cm^{-1} are shown over a limited pressure range due to the overlap with the diamond mode. The prime symbol denotes modes that either overlap with other modes at 0.6 GPa or show up at higher pressures.

polymorph is stable across a wide pressure range. However, with decreasing pressure (<0.6 GPa) the Raman spectra revert to that of the α-phase. The pressure dependencies of the Raman shifts (dν/dp: pressure coefficient) were obtained from the least-squares fits of the experimental data to either a linear or a polynomial equation. Table 1 includes the calculated coefficients at 0.6 and 20 GPa together with the tentative mode assignments and their frequencies.

3.2.2. Frequency Range 1700−1100 cm^{-1} (Contributions from NO_2, NN, and CNC Stretching and CH_2 Wagging Modes). The pressure effects on Raman spectra in this frequency range are shown in Figures 5 and 6. All modes in this range, with the exception of one at 1578 cm^{-1}, have relatively low intensities. Note that the modes near 1332 cm^{-1} were either not measured or were measured in a limited pressure region due to an overlap with a strong Raman peak from the diamond anvils. Several features are apparent in this pressure range: (i) changes in the relative intensities of some Raman modes, (ii) different pressure shifts for different groups of vibrations, and (iii) increased separation as well as disappearance of some of the N−N stretching modes. Among the modes in this range, the smallest shifts were observed in N−N stretching modes, moderate shifts for NO_2 stretching modes, and largest shifts for the CNC stretching and CH_2 modes. The most interesting behavior is that of the N−N stretching modes between 1400 and 1500 cm^{-1}. Details of the pressure effect on these modes are shown in panel B of Figure 5. Three peaks, ν_{12}, ν_{13}, and ν_{14}, can be resolved from the spectrum at low pressures. However, as pressure increases, the envelope of these modes undergoes significant transformations. First, the ν_{12} mode separates into two modes at ∼3 GPa and then vanishes into the spectrum background. In contrast, the new emerging mode, ν'_{12}, significantly gains intensity as pressure increases. At the same time, the strong ν_{13} mode gradually loses intensity. Above 9 GPa, a new peak, designated ν'_{13}, shows up between the ν_{13} and ν_{14} modes. This complex evolution of peaks associated with the N−N stretching vibrations likely indicates: (i) a change in molecular and/or crystal symmetry as a result of the phase transformation, (ii) an increased contribution of factor group splitting due to increased pressure, or (iii) the modification of molecular structure within the same molecular symmetry. At present, it is unclear which of these mechanisms causes the observed changes in the N−N stretching modes.

3.2.3. Frequency Range 1100−350 cm^{-1} (Contributions from the CH_2 Rocking, N−NC_2 and N−NO_2 Umbrella, and Various Ring Modes). Figures 7 and 8 present pressure-induced changes in the Raman modes located in the frequency range of 1100 to 350 cm^{-1}. Examination of the spectra and Raman shifts show that: (i) some of the peaks occur as doublets, (ii) the N-NO_2 umbrella mode, ν_{33}, has a negative pressure dependence of Raman shift at lower pressures, and (iii) the peaks labeled ν_{33} (N-NO_2 umbrella), ν_{39} (N-NC_2 umbrella), and ν_{40} (ring bending) split around 3 GPa. Note that this splitting involves vibrations associated with the triazine ring and leads to a rather small separation of peaks. Furthermore, the splitting of these peaks coincides with the disappearance of peak ν_{12} and the appearance of peak ν'_{12}.

3.2.4. Frequency Range 50−350 cm^{-1} (Contributions from the Ring, Various NO_2, and Lattice Modes). Figures 9 and 10 present Raman spectra and pressure shifts in the low frequency range, including the lattice modes. As shown in Table 1, with exception of one mode, all Raman shift pressure dependencies in this frequency range are positive, varying from 4 to 14 (cm GPa^{-1}), with larger values <160 cm^{-1}. The mode with a negative shift, ν_{41}, is associated with the triazine ring stretching vibrations. However, the negative shift of this mode converts to a positive shift at about 2 GPa. This is similar to the behavior observed for the N−NO_2 umbrella vibrations, the ν_{33} mode. In both cases, the sign of the Raman modes shift changes from negative to positive at the same pressure. The coincidence of changes in the behavior of the vibration of the ν_{41} and ν_{33} modes may indicate alterations in the triazine ring at ∼2 GPa.

To distinguish between internal and external (lattice) modes in the HP−HT polymorph, we utilized the vibrational scaling

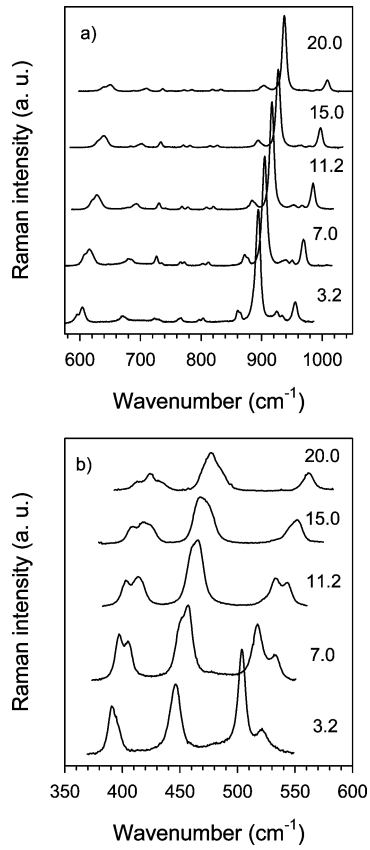

Figure 7. Raman spectra at several pressures in the frequency range: (a) 600−1000 cm^{-1}, CH_2 rocking and ring modes and (b) 350−600 cm^{-1}, ring modes.

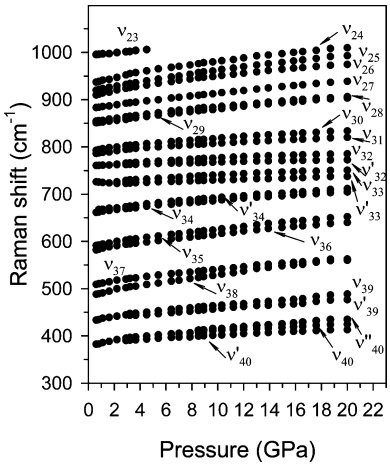

Figure 8. Pressure-induced shift of Raman modes between 350 and 1000 cm^{-1}. Prime or double prime symbols denote modes that either overlap with other modes at 0.6 GPa or show up at higher pressures.

law (VSL) that was effectively used for molecular crystals.[24,25] According to VSL, the log−log plot of relative pressure coefficients of Raman modes, $\nu^{-1}d\nu/dp$, versus mode frequency, ν, both taken under ambient conditions should yield two straight lines. The two lines, with slopes of 1 and −2 superimposed on the data, represent the main trends of the overall behavior of the lattice and intramolecular modes, respectively. In Figure 11, we plot the data for the HP−HT polymorph obtained at 0.6 GPa, the lowest pressure at which this polymorph exists. It is clear that these data can be approximated by two straight lines. The first line, with a slope of −2, fits the high frequency data

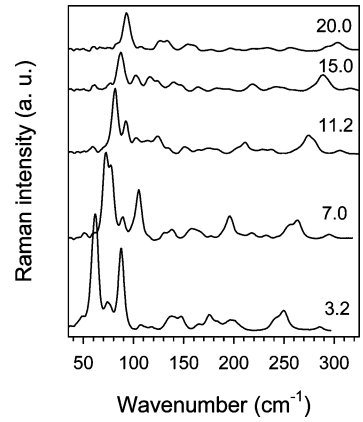

Figure 9. Raman spectra in the frequency range 20−350 cm^{-1} at several pressures; pressure effects on the ring, NNC_2 umbrella, NO_2 rotation, and lattice vibrations.

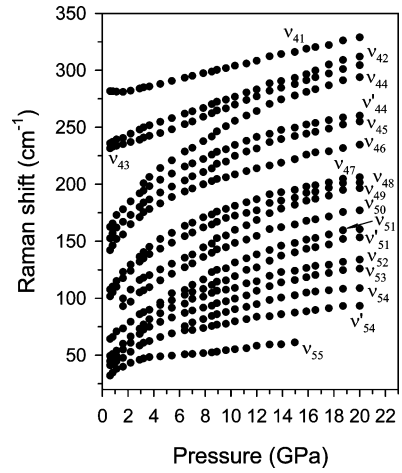

Figure 10. Pressure-induced shift of Raman modes between 20 and 350 cm^{-1}. Prime symbol denotes modes that either overlap with other modes at 0.6 GPa or show up at higher pressures.

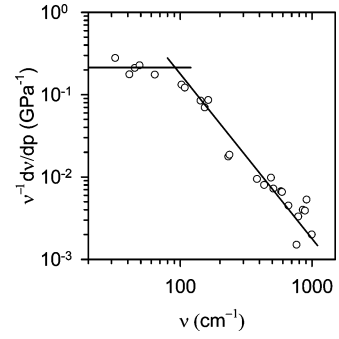

Figure 11. Plot of relative pressure coefficients, $\nu^{-1}d\nu/dp$, as a function of mode frequency, ν. The two lines, with slopes 1 and −2, represent the trends in the lattice and intramolecular modes with pressure. Intersection of the two lines marks the high-frequency end of the lattice modes.

and intersects the horizontal line at the high-frequency end of the lattice modes; the horizontal line was set at the mean value of $\nu^{-1}d\nu/dp$ in the low-frequency region. The intersection indicated that modes below ∼90 cm^{-1} can be considered as lattice modes. In the next subsection, we discuss this issue further in relation to the crystal structures of α- and γ-RDX.

3.3. Comparison between Different RDX Polymorphs. ***3.3.1. α, γ, and HP−HT Polymorphs.*** To assess the link between the HP−HT polymorph and other RDX polymorphs, we compared their vibrational spectra under analogous condi-

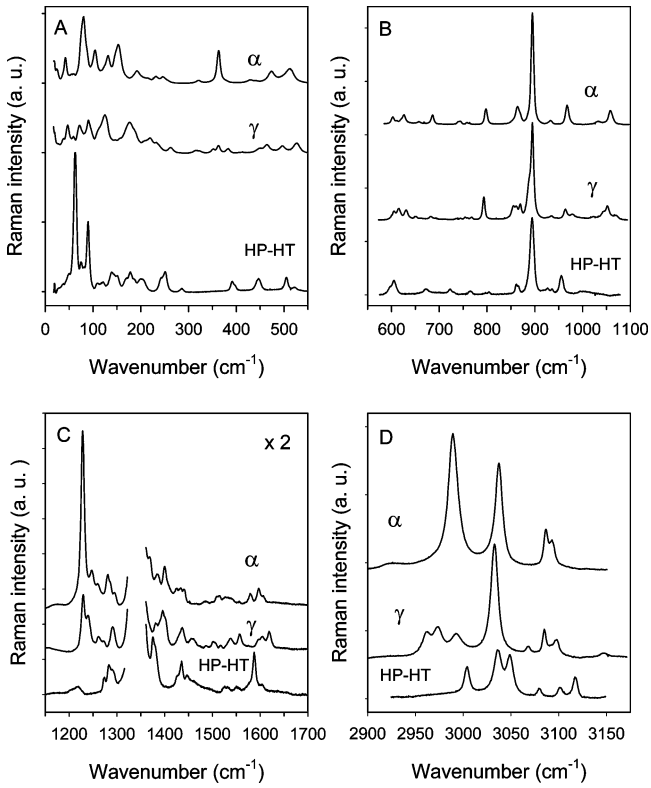

Figure 12. Comparison of Raman spectra of three RDX polymorphs at high pressures obtained for the same sample at room temperature: α-RDX at 3.6 GPa, γ-RDX at 3.8 GPa, and HP−HT RDX at 3.8 GPa (±0.1 GPa). The four panels show spectra in different frequency ranges: (A) 20−550; (B) 600−1100; (C) 1150−1700 cm^{-1}, spectra in this range were magnified by a factor of 2; (D) 2900−3150 cm^{-1}.

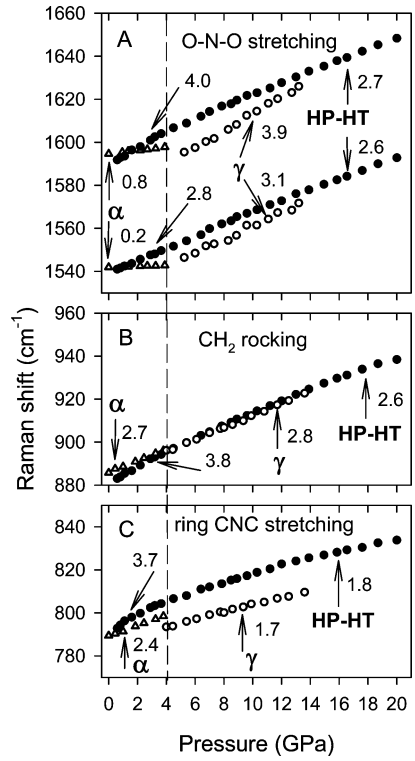

Figure 13. Pressure-induced shifts of selected Raman modes for three RDX polymorphs: (△) α-RDX, (○) γ-RDX, and (●) HP−HT RDX. Panels present: (A) NO_2 stretching modes, (B) CH_2 rocking mode, and (C) ring CNC stretching mode. Approximated pressure coefficients ($d\nu/dp$) were calculated from the linear fits for each polymorph. The vertical dashed line marks the onset of the transition from α-RDX to γ-RDX. Data for α- and γ-RDX are from ref 2.

tions. In Figure 12, we present a wide range of Raman spectra (30 to 3200 cm^{-1}) for the α, γ, and HP−HT polymorphs. These spectra were obtained with the same sample undergoing the following treatment: (1) application of pressure to 3.6 GPa (α-RDX), (2) increase of pressure to 3.8 GPa (γ-RDX), and (3) heating to 473 K, followed by instantaneous cooling to 293 K (HP−HT RDX). Upon quenching of the HP−HT polymorph to room temperature, the pressure was maintained within ±0.1 GPa. It is clear that the spectra for the three polymorphs differ significantly over all frequency ranges.

We focus on the comparison of the HP−HT polymorph spectrum with the spectra of the α- and γ-polymorphs. Several observations are in order regarding the HP−HT polymorph: (i) shifting of low frequency modes toward higher frequencies with respect to α- and γ-polymorphs, (ii) vanishing of modes in several frequency ranges: 300−400, 600−650, 1000−1100, 1200−1250, and ∼1400 cm^{-1}, and (iii) shifting of CH stretching modes toward higher frequencies with respect to the α- and γ-polymorphs. Overall, the HP−HT polymorph spectra differ more from the spectra of the α- and γ-polymorphs than the last two differ from each other.

In Figure 13, we compare the pressure-induced shifts of the Raman modes for the three polymorphs. Three typical modes are illustrated: NO_2 stretching, CH_2 rocking, and ring CNC stretching vibrations. There is clearly a large difference between the pressure coefficients for the HP−HT and the α-polymorphs, regardless of mode type. In contrast, the pressure coefficients are quite similar for the HP−HT and γ-polymorphs. This result indicates that the pressure-induced changes in intramolecular interactions in the HP−HT polymorph are comparable to those in the γ-polymorph and not the α-polymorph.

In Figure 14, we compare the Raman spectra of the three polymorphs in the frequency range related to lattice modes. The assignment and pressure dependencies of lattice modes in α-RDX are well established.[2,26,27] Of the 24 Raman active modes predicted by group theory for the *Pbca* space group, only 9 are detected under ambient conditions. All of these modes occupy a narrow frequency range of ∼120 wavenumbers at 3.6 GPa. (See Figure 14.) Similarly, γ-RDX, with the same number of molecules in the unit cell, exhibits only 10 Raman peaks from the 21 predicted for the $Pca2_1$ space group. The pattern of the low-frequency modes for the HP−HT polymorph differs considerably from that of the other two polymorphs: (i) the lowest detected frequency of the HP−HT RDX is higher than the lowest frequencies of the α- or γ-RDX, (ii) the low frequency modes for the HP−HT polymorph are better separated from each other than modes in the other two polymorphs, and (iii) fewer Raman peaks are observed for the HP−HT polymorph than in the two others polymorphs.

3.3.2. β-Polymorph versus HP−HT Polymorph. The HP−HT polymorph was initially thought to be the β-polymorph.[18,19] We examine this suggestion by comparing the Raman spectrum for the HP−HT polymorph and the Raman spectra for the β-polymorph in Figure 15. Spectrum for the HP−HT polymorph was obtained at 0.8 GPa. Spectra for the β-polymorph are at ambient pressure. They correspond to present measurements on single crystal prepared from a highly concentrated solution of nitrobenzene (red line in Figure 15) and values from Table 1 of ref 16 (green lines). The numerical values of the Raman peaks for the HP−HT and β-polymorphs obtained by two different methods are listed in Table 1.

First, there is good agreement in the position of Raman modes obtained for β-RDX using different methods. Second, as

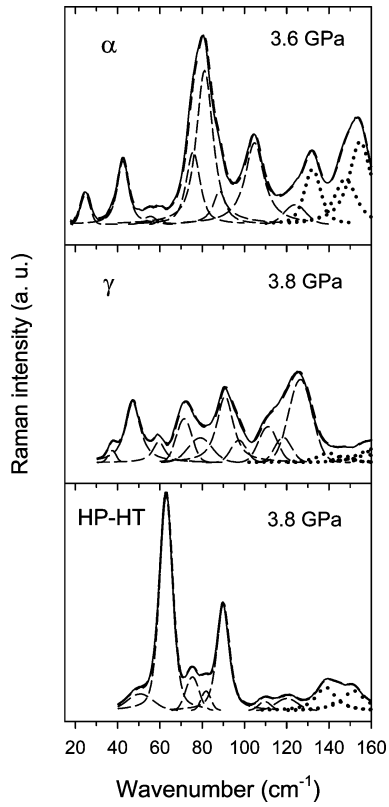

Figure 14. Example of separation of vibrational modes from the low frequency Raman spectra of α-RDX, γ-RDX, and HP−HT RDX. External modes are denoted by dashed lines and internal modes are denoted by dotted lines. The assignments of lattice modes for the α- and γ-polymorphs are based on refs 2, 26, and 27, and the assignment for the HP−HT polymorph is based on the considerations presented in Section 3.2.4.

expected, the Raman peaks of the HP−HT polymorph are somewhat shifted to higher frequencies with respect to the corresponding peaks of β-RDX because of the fact that the spectrum of the HP−HT polymorph was obtained at 0.8 GPa and the spectrum of β-RDX was obtained at ambient pressure. Third, the spectrum of the HP−HT polymorph seems to be in general agreement with the spectrum of the β-polymorph. However, a careful examination reveals several noticeable differences. The most significant difference is in the pattern of the lattice modes. Also, a number of Raman peaks observed for the HP−HT RDX have no correspondence in the spectrum of β-RDX. Some of these modes are: ν_3, ν_4, and ν_6 (CH st); ν_{14} and ν_{16} (N−N st); ν_{22} (CNC st); ν_{25} (CH_2 r); ν_{36} (ring vibrations); ν_{44} and ν_{46} (NO_2 rot); and ν_{51} and ν_{54} (lattice). Furthermore, contrary to expectation, several peaks in the HP−HT polymorph (for example ν_{10}, ν_{23}, and ν_{33}) occur at lower frequencies than the corresponding peaks of the β-polymorph. Also, the relative intensities of the Raman peaks for the two polymorphs disagree somewhat. Because of these differences, we believe that the HP−HT and the β-polymorphs correspond to different structures.

3.4. Discussion on the HP−HT Polymorph Stability and Structure. Up to 20 GPa, the Raman spectra measurements for the HP−HT polymorph revealed gradual shifts in most modes. This indicates that the HP−HT polymorph is structurally stable over a wide pressure range (0.6 GPa to at least 20 GPa). However, it should be pointed out that some exceptions to this behavior were observed: (i) negative pressure shifts initially for the ν_{33} and ν_{41} modes, (ii) occurrence of new peaks as a result of splitting of the ν_{39} and ν_{40} modes, and (iii) development of new peaks: ν'_{12}, ν_{49}, and ν_{50}. All of these changes arise at about 2 to 3 GPa. Because only a few new peaks occur and because it happens gradually and in close proximity to other peaks, it seems unlikely that these new features indicate a phase transformation. The reason for the occurrence of these new peaks is unclear. However, contributing factors may include: (i) separation of peaks with increasing pressure that are otherwise overlapped at low pressure, (ii) separation of peaks due to the increased role of factor group splitting, and (iii) perturbation of the sample due to solidification/melting of argon at ∼2 GPa.

The Raman spectra of the HP−HT polymorph, presented here, indicate that this polymorph has different structure than other studied polymorphs. It is clearly demonstrated by differences in both the intramolecular and lattice mode patterns. Whereas a structure of the HP−HT polymorph cannot be determined solely from the Raman measurements, it is worthwhile to narrow down the list of likely candidates.

From analyses of the intramolecular modes spectra, we find that the HP−HT polymorph has fewer Raman peaks than the α-polymorph and more than the β-polymorph. Specifically, several modes located at 347, 607, 1031, 1232, and 1388 cm^{-1} in the spectrum of α-polymorph disappear from the spectrum of the HP−HT polymorph. All of these modes are assigned to A″ symmetry.[2,5] It can be shown that the disappearance of the

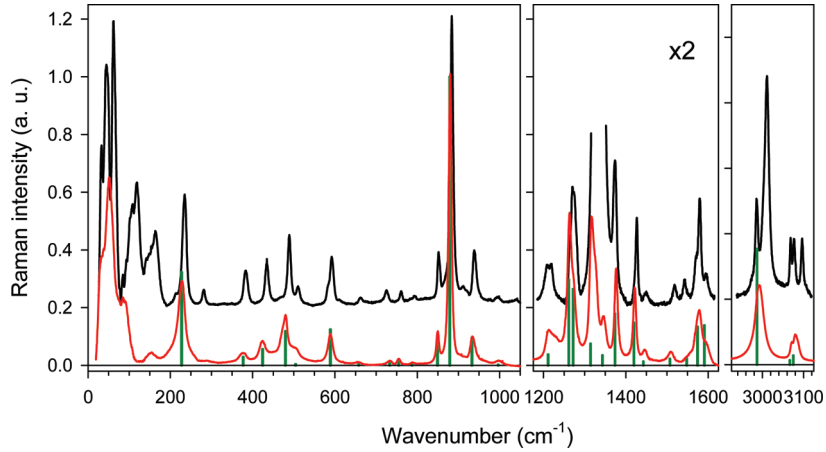

Figure 15. Comparison between Raman modes of the HP−HT RDX and β-RDX. The HP−HT RDX spectrum, shifted for clarity, is represented by a dark line and was obtained at 0.8 GPa and room temperature. The β-RDX spectra (obtained at ambient pressures) are: (a) data taken from Table 1 in ref 16 and represented by a green line and (b) from this work represented by a red line. Intensities of Raman peaks are related to the strongest peak located at 883 cm^{-1}. The intensities of Raman modes in the range from 1200 to 1600 cm^{-1} are multiplied by 2.

A″ is consistent with the increase of molecular symmetry from C_s to C_{3v}. In this case, some of the A″ modes that are Raman active will transform to A_2 modes that are Raman inactive.[28] The C_{3v} molecular symmetry in RDX is commonly attributed to the AAA molecular conformer; all nitro-groups are in the axial position with respect to the triazine ring. This conformer has already been proposed to be adopted in solution[29] and vapor[30] phases of RDX. Recently, it was shown that the AAA conformer is also adopted in the β-polymorph.[16,17] One would expect, then that molecules in the HP−HT polymorph assume the AAA conformation as well. However, careful comparison of the vibrational spectrum of the HP−HT polymorph with the vibrational spectrum of the β-polymorph (Figure 15) clearly shows differences between the two spectra. The most pronounced is the difference in the CH stretching modes; this likely indicates a different arrangement of the CH bonds with respect to the triazine ring in the HP−HT and β-polymorphs. Therefore, we propose that molecules in the HP−HT polymorph assume the pseudo-AAA conformations rather than the AAA-conformation, due to the alterations in the CH bonding arrangement.

Further information on the possible structure of the HP−HT polymorph is obtained from the inspection of Raman spectra in the low-frequency range. The examination indicates that the HP−HT polymorph has fewer lattice modes than the α-, γ-, or β-polymorphs. The decrease in the number of lattice modes in the Raman spectra is in general indicative of the increasing of crystal symmetry or decreasing of molecules number in the unit cell. Because the α-, γ-, and β-polymorphs all have the orthorhombic structures with eight molecules in the unit cell, it is reasonable to assume that the HP−HT polymorph has either tetragonal structure with eight molecules or orthorhombic with four molecules. Furthermore, if one takes into account that the C_{3v} molecular symmetry in the tetragonal and orthorhombic structures can only be accommodated on the C_1 site symmetry, then the following structures are consistent with our assumptions: tetragonal (C_{4h}, D_4, C_{4v}, D_{2d}, D_{4h}) or orthorhombic (D_2, C_{2v}).[28]

It is expected that the Raman and infrared (IR) vibrations should be coincidental only for the C_{2v} factor group. Comparison of our Raman spectra with the available IR spectra in the region of CH stretching modes[19] indicates a reasonable agreement between the frequencies of peaks in both spectra. Given that, we propose that the space group of the HP−HT polymorph can be isomorphous with the $C_{2v}[C_1(4)]$ point group and that four molecules in the unit cell assume the pseudo-AAA conformations. Furthermore, the comparable pressure coefficients of Raman modes in the HP−HT polymorph and γ-polymorph suggest similar changes in the intermolecular interactions and, therefore, comparable packing of molecules in these two polymorphs. Therefore, these results indicate that the structures of the HP−HT and β-polymorphs are different. The possibility of different structure for the HP−HT and β-polymorph was also recently suggested in ref 17. Our Raman studies confirm this suggestion and provide additional information on the possible structure of the HP−HT polymorph. Therefore, we agree with authors of ref 17 that the HP−HT polymorph should be given a separate designation, ε-RDX, to distinguish it from the β-RDX. Ultimately, X-ray diffraction measurements on the single crystal will be required to determine the exact structure of the HP−HT polymorph (ε-RDX).

4. Summary and Conclusions

We performed Raman measurements over a wide range of pressures on the HP−HT polymorph of RDX crystal quenched to room temperature. Although this polymorph has limited chemical stability under the elevated temperatures and pressures where it is produced, we show that it is chemically and structurally stable from 0.6 GPa to at least 20 GPa at room temperature. Below 0.6 GPa, the HP−HT polymorph reverts to the α-polymorph that exists under ambient conditions. Pressure effects on the Raman spectrum of the HP−HT polymorph were examined, and detailed changes in both the internal and external vibrations were determined. The pressure coefficients of Raman modes in the HP−HT polymorph are comparable to those in the γ-polymorph. Comparison of vibrational spectra of the HP−HT polymorph with other RDX polymorphs indicates clear differences between the HP−HT polymorph and other polymorphs. In contrast with previous suggestions, our results suggest that the HP−HT polymorph likely has a different structure than the β-polymorph. As such, it should be given a separate designation: ε-RDX.[17] We propose that the molecules in the ε-polymorph can assume pseudo-AAA conformations and the space group of this polymorph can be isomorphous with the $C_{2v}[C_1(4)]$ point group. Finally, we point out that the obtained pressure effects on the vibrational structure of ε-RDX can be utilized for understanding the structural and chemical processes occurring in the shocked RDX crystal.

Acknowledgment. Dr. D. E. Hooks from Los Alamos is thanked for providing the RDX crystals. This work was supported by ONR-MURI grant N00014-06-1-0459 and DOE grant DEFG0397SF21388.

References and Notes

(1) Hooper, J. *J. Chem. Phys.* **2010**, *132*, 014507.
(2) Dreger, Z. A.; Gupta, Y. M. *J. Phys. Chem. B* **2007**, *111*, 3893.
(3) Dreger, Z. A.; Patterson, J. E.; Gupta, Y. M. *J. Phys.: Conf. Ser.* **2008**, *121*, 042012.
(4) Patterson, J. E.; Dreger, Z. A.; Gupta, Y. M. *J. Phys. Chem. B* **2007**, *111*, 10897.
(5) Miao, M. S.; Dreger, Z. A.; Winey, J. M.; Gupta, Y. M. *J. Phys. Chem. A* **2008**, *112*, 12228.
(6) Dreger, Z. A.; Gupta, Y. M., submitted.
(7) Patterson, J. E.; Dreger, Z. A.; Miao, M. S.; Gupta, Y. M. *J. Phys. Chem. A* **2008**, *112*, 7374.
(8) Miao, M. S.; Dreger, Z. A.; Patterson, J. E.; Gupta, Y. M. *J. Phys. Chem. A* **2008**, *112*, 7383.
(9) McCrone, W. C. *Anal. Chem.* **1950**, *22*, 954.
(10) Choi, C. S.; Prince, E. *Acta Crystallogr., Sect. B* **1972**, *28*, 2857.
(11) Olinger, B.; Roof, B; Cady, H. In *Proceedings of International Symposium on High Dynamic Pressures*; C.E.A.: Paris, 1978; p 3.
(12) Davidson, A. J.; Oswald, I. D. H.; Francis, D. J.; Lennie, A. R.; Marshall, W. G.; Millar, D. I. A.; Pulham, C. R.; Warren, J. E.; Cumming, A. S. *CrystEngComm.* **2008**, *10*, 162.
(13) Ciezak, J. A.; Jenkins, T. A.; Liu, Z.; Hemley, R. J. *J. Phys. Chem. A* **2007**, *111*, 59.
(14) Karpowicz, R. J.; Sergio, S. T.; Brill, T. B. *Ind. Eng. Chem. Prod. Res. Dev.* **1983**, *22*, 363.
(15) Karpowicz, R. J.; Brill, T. B. *J. Phys. Chem.* **1984**, *88*, 348.
(16) Torres, P.; Mercado, L.; Cotte, I.; Hernandez, S. P.; Mina, N.; Santana, A.; Chamberlain, R. T.; Lareau, R.; Castro, M. E. *J. Phys. Chem. B* **2004**, *108*, 8799.
(17) Millar, D. I.; Oswald, I. D. H.; Francis, D. J.; Marshall, W. G.; Pulham, C. R.; Warren, J. E.; Cumming, A. S. *Chem. Commun.* **2009**, 562.
(18) Baer, B. J.; Oxley, J.; Nicol, M. *High Pressure Res.* **1990**, *2*, 99.
(19) Miller, P. J.; Block, S.; Piermarini, G. J. *Combust. Flame* **1991**, *83*, 174.
(20) Rice, M. B.; Chabalowski, C. F. *J. Phys. Chem. A* **1997**, *101*, 8720.
(21) Vladimiroff, T.; Rice, B. M. *J. Phys. Chem. A* **2002**, *106*, 10437.
(22) Barnett, J. D.; Block, S.; Piermarini, G. J. *Rev. Sci. Instrum.* **1973**, *44*, 1.
(23) Park, T. R.; Dreger, Z. A.; Gupta, Y. M. *J. Phys. Chem. B* **2004**, *108*, 3174.
(24) Zallen, R. *Phys. Rev. B* **1974**, *9*, 4485.
(25) Zallen, R.; Slade, M. L. *Phys. Rev. B* **1978**, *18*, 5775.
(26) Rey-Lafon, M.; Cavagnat, R.; Trinquecoste, C.; Forel, M. T. *J. Chim. Phys. Phys.−Chim. Biol.* **1971**, *68*, 1575.

(27) Haycraft, J. J.; Stevens, L. L.; Eckhardt, C. J. *J. Appl. Phys.* **2006**, *100*, 053508.

(28) Fateley, W. G.; Dillish, F. R.; McDevitt, N. T.; Bentley, F. F. *Infrared and Raman Selection Rules for Molecular and Lattice Vibrations: The Correlation Method*; J. Wiley & Sons: New York, 1972.

(29) Karpowicz, R. J.; Sergio, S. T.; Brill, T. B. *Ind. Eng. Chem.* **1983**, *22*, 363.

(30) Shishkov, L. F.; Vilkov, L. V.; Kolonits, M.; Rozsondai, B. *Struct. Chem.* **1990**, *2*, 57.

JP102668D